20th IMEKO TC4 International Symposium and
18th International Workshop on ADC Modelling and Testing
Research on Electric and Electronic Measurement for the Economic Upturn
Benevento, Italy, September 15-17, 2014

New generation of cage-type current shunts at CMI

Věra Nováková Zachovalová[1], Martin Šíra[1], Pavel Bednář[1]

[1] *Czech Metrology Institute, Okruzni 31 638 00 Brno, Czech Rep., vnovakovazachovalova@cmi.cz*

***Abstract* – This paper describes a new generation of cage-type ac/dc current shunts from 30 mA up to 10 A developed using a lumped circuit element model. Comparison of the calculated and measured values shows agreement better than 6 μΩ/Ω in the ac-dc difference at frequencies up to 100 kHz.**

I. INTRODUCTION

In recent years the shunts of special designs for high accuracy current measurement were developed at several national metrology institutes (NMI) [1-8].

In previous research a calculable model of the CMI cage shunts was developed using lumped circuit elements. The transimpedance, ac-dc difference and also the phase angle error of a shunt can be derived from the model [9].

The goal of this research was to build new generation of the cage shunts from 30 mA up to 10 A based on the model calculation.

II. CAGE-TYPE CURRENT SHUNTS CONSTRUCTION

The physical design of the original CMI's shunts is shown in Fig. 1 (detailed in Fig.2).

The shunts are constructed using single-sided and double-sided fibreglass-epoxy PCB material (FR4 with permittivity 5.45 and loss factor 0.0205) of 2 mm thickness with mounted Vishay foil Z201 or S102 resistors and can be split in the following construction parts [7, 9]:

- input connector,
- input part (two disks made of single-sided PCB),
- crossbars made of double-sided PCB,
- resistors,
- output part (circle and disk made of single-sided PCB and an aluminum wire connected between circle and output connector),
- output connector.

The input connector brings the current to the input disks, which spread the current through the crossbars. Each crossbar carry a fraction of the input current to resistors connected in parallel. The output part senses the voltage drop across the resistors. The number, value and type of resistors are different in each shunt (Table 1) [7].

Fig. 1. The original CMI shunts

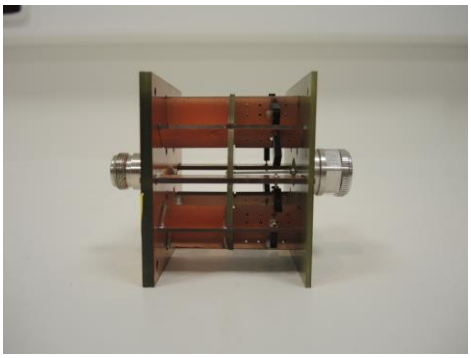

Fig. 2. The design of original 100 mA shunt

Table 1.General parameters of the original shunts.

Nominal current	Resistance (Ω)	Number and value of resistors	Type of resitors	PCB type
30 mA	50	3x 150 Ω	Z201	FR4
100 mA	10	10x 100 Ω	3x S102C 7x S102K	FR4
300 mA	3.3	30x 100 Ω	10x S102C 20x S102K	FR4
1 A	1	100x 100 Ω	33x S102C 67x S102K	FR4
10 A	0.1	100x 10 Ω	33x S102C 67x S102K	FR4

ISBN-14: 978-92-990073-2-7

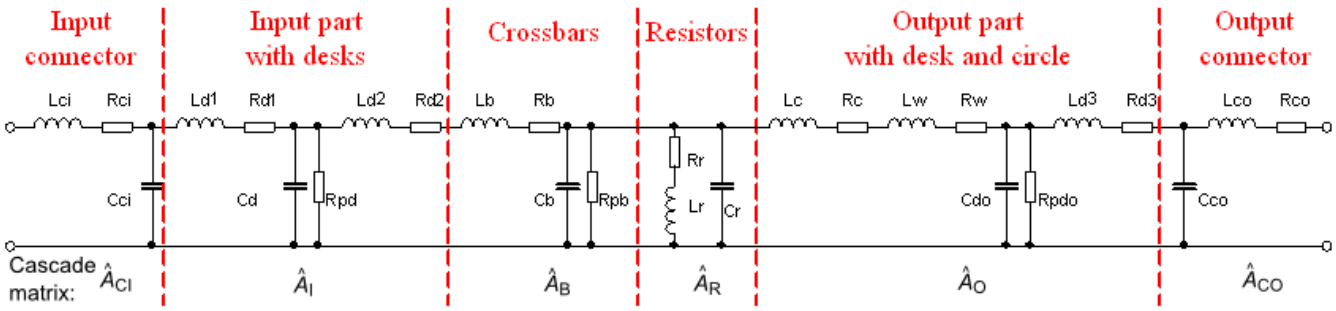

Fig. 3. Lumped element model of the shunts

The temperature coefficient of the shunts was reduced by using a suitable combination of resistors S102 with different temperature coefficients (1/3 of S102C a 2/3 of S102K), except 30 mA shunt with Z201 resistors, which temperature coefficient is below 1 ppm/K [7].

These shunts were developed to be suitable for use with planar multijunction thermal converters (PMJTC). The voltage drop across every shunt in parallel with a 90 Ω PMJTC is 1 V at nominal current [7, 8].

III. LUMPED CIRCUIT ELEMENT MODEL OF THE SHUNTS

The shunts model is made by cascade concatenation of circuit elements two-ports assigned to the construction parts (see Fig. 3) [9].

The product of the cascade matrixes of the two-ports defines the cascade matrix of the model [9]:

$$\hat{A}_{S} = \hat{A}_{CI}\hat{A}_{I}\hat{A}_{B}\hat{A}_{R}\hat{A}_{O}\hat{A}_{CO} \qquad (1)$$

During measurements the output of the shunt is loaded by the device measuring the voltage drop across the shunt. Therefore it is necessary to include this load into the model. Than, the cascade matrix of the loaded shunt model is [9]:

$$\hat{A} = \hat{A}_{S}\hat{A}_{L} = \begin{bmatrix} \hat{a}_{11} & \hat{a}_{12} \\ \hat{a}_{21} & \hat{a}_{22} \end{bmatrix}, \qquad (2)$$

where $\hat{A}_{L}$ is cascade matrix assigned to the load [9].

From the cascade matrix of the model the transimpedance of the shunt can be calculated [9]:

$$\hat{Z}_{T} = \frac{1}{\hat{a}_{21}} \qquad (3)$$

From the transimpedance the phase-angle error and ac-dc difference can be derived easily [9].

This model is based on calculations of all component values from the geometry and material properties. Therefore it was necessary to be familiar with the dielectric properties of the PCB (permittivity, loss factor) and capacitance and inductance of the resistor, which had to be measured [9].

Evaluation of associated uncertainties of the model was done by means of Monte Carlo methods [9].

Detailed description of model calculation is given in [9].

Comparison of the calculated and measured values showed agreement better than 6 μΩ/Ω in the ac-dc difference and 110 μrad in the phase angle error at frequencies up to 100 kHz [9].

IV. CONSTRUCTION IMPROVEMENTS

The shunts model can be used to determine the sensitivity of the output quantities to the modification of the input quantities, resulting in improvements to the construction of the shunts [9].

A. Theoretical analysis

The sensitivity of the calculated values of the ac-dc difference and phase angle error to modification of the input quantities of the model was investigated using parametric simulation and is described in [9] in detail.

Calculations indicated that some of the input quantities have significant influence and some of the input quantities have insignificant influence on the calculated values of the ac-dc difference and phase angle error. Following input quantities of the model were found to have significant influence on the calculated values [9]:

- capacitance and inductance of resistors,
- relative permittivity and loss factor of PCB,
- thickness of PCB,
- number of crossbars and geometric dimensions.

Calculations also indicated that the sensitivities of the calculated values of the ac-dc difference and phase angle error with respect to modification of these model input quantities are different for the low-current and high-current shunts construction.

The dielectric properties and thickness of PCB are input quantities affecting the ac-dc difference of the low-current shunts, while the ac-dc difference of high-current shunts depends more on the geometric dimensions and less on the dielectric properties and thickness of the PCB [9].

The phase angle error of the low-current shunts is influenced by dielectric properties and thickness of PCB and also by geometric dimensions. The phase angle error of high-current shunts is affected mainly by the inductances of resistors, but also slightly by the geometric dimensions [9].

B. Construction of the new generation cage-type current shunts

Figure 4 shows the new generation of cage-type shunts from 30 mA up to 10 A developed at CMI. The voltage drop across every shunt is 0.6 V at nominal current to be convenient for use with PMJTC and also with sampling wattmeter.

The improvements to the shunts construction resulted from the theoretical analysis based on the lumped element model and described above. General information about resistors and PCB material used for their construction are in Table 2.

The low current shunts (up to 1 A) were constructed using high frequency PCB material RO4350B with better dielectric properties (permittivity = 3.6, loss factor = 0.0031) than previously used FR4 material. Thickness of PCB was reduced from 2 mm down to 1.524 mm. Geometrical dimension should be kept as small as possible to obtain low frequency dependence of shunts transimpedance. The dimensions of the 30 mA shunt were slightly reduced to be the same as for the 100 mA shunt. Also number of crossbars was minimized only to three and the 30 mA shunt construction was reinforced using distance struts. The dimensions of the 100 mA, 300 mA and 1 A shunts were not modified. The length of the crossbars was reduced in all shunts.

10 A shunt was constructed using low frequency PCB (FR4) because of inconsiderable influence of its dielectric properties to the calculated values. Only the thickness of the FR4 was reduced to 1.5 mm. Dimensions of 10 A shunt were reduced to be same as the original 1 A shunt. The length of the crossbars was also reduced to be as short as possible.

Resistors mounted in the shunts are the same type as in previous construction because no other resistors with lower inductance were found.

Including all of these modifications into the model showed a reduction in the ac-dc difference below 3.5 μΩ/Ω at frequencies up to 100 kHz (see Table 3).

V. COMPARISON OF CALCULATED AND MEASURED VALUES

The ac-dc difference of the shunts was measured using an automated measurement system of ac-dc current transfer difference step up (see Fig. 5). A reference and a calibrated standard are connected in series. Ac and

Fig. 4. New generation of cage-type shunts.

Table 2.General parameters of the new shunts.

Nominal current	Resistance (Ω)	Number and value of resistors	Type of resitors	PCB type
30 mA	20	3x 60 Ω	Z201	RO4350B
100 mA	6	10x 60 Ω	3x S102C 7x S102K	RO4350B
300 mA	2	30x 60 Ω	10x S102C 20x S102K	RO4350B
1 A	0.6	50x 30 Ω	17x S102C 33x S102K	RO4350B
10 A	0.06	100x 6 Ω	33x S102C 67x S102K	FR4

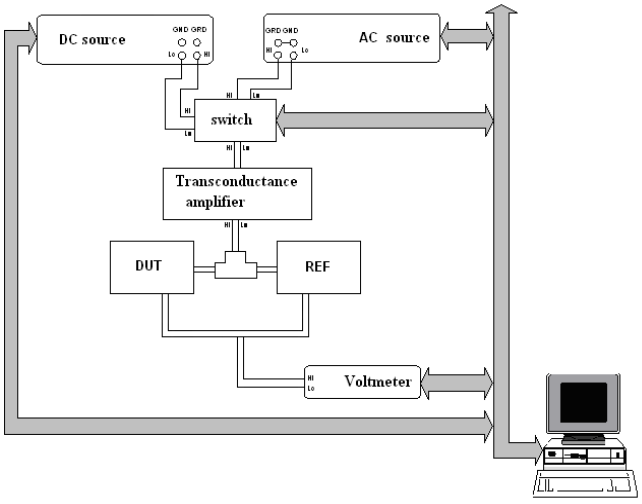

Fig 5. Measurement system of ac-dc current transfer difference.

dc currents are applied through a transconductance amplifier, which is alternately connected to dc and ac voltage source using an automated switch. The standards are comprised of a shunt loaded by a thermal converter [7, 8].

During the measurements of the new generation of the shunts the output of the shunts was loaded by a 90 Ω/10 mA planar multijunction thermal converter, which was considered in the model.

Table 3 shows agreement between the measured and calculated values of the ac-dc differences of the new generation of the shunts to be better than 6 μΩ/Ω at frequencies up to 100 kHz.

Table 4 shows comparison of measured ac-dc differences of the original and new shunts. Most significant reducing of ac-dc difference (more than 100 μΩ/Ω) was achieved for the 30 mA shunt.

VI. CONCLUSION

A new generation of cage-type current shunts from 30 mA up to 10 A was developed.

Construction improvements were done based on results obtained from the analysis of the lumped element model of the original shunts.

Table 3.Calculated and measured values of the ac-dc difference for the new shunts with associated uncertainties for k=1.

Shunt	Value	Ac-dc difference	Frequency					
			500 Hz	1 kHz	10 kHz	20 kHz	50 kHz	100 kHz
30 mA	20 Ω	Calulated (μΩ/Ω)	0.016	0.032	0.320	0.650	1.700	3.400
		Unc. (μΩ/Ω)	0.005	0.010	0.096	0.190	0.490	0.980
		Measured (μΩ/Ω)	-0.4	-0.5	1.5	2.9	4.7	7.0
		Unc. (μΩ/Ω)	4.4	4.4	4.4	4.4	4.4	4.7
100 mA	6 Ω	Calulated (μΩ/Ω)	0.011	0.022	0.022	0.440	1.110	2.240
		Unc. (μΩ/Ω)	0.003	0.007	0.067	0.130	0.340	0.680
		Measured (μΩ/Ω)	-0.9	-1.7	0.7	3.4	4.4	6.4
		Unc. (μΩ/Ω)	6.4	6.4	6.4	6.5	6.7	7.1
300 mA	2 Ω	Calulated (μΩ/Ω)	0.004	0.008	0.075	0.150	0.350	0.620
		Unc. (μΩ/Ω)	0.001	0.002	0.023	0.047	0.120	0.230
		Measured (μΩ/Ω)	0.9	1.1	1.1	1.9	4.3	5.5
		Unc. (μΩ/Ω)	7.9	7.9	7.9	8.0	8.4	8.9
1 A	0.6 Ω	Calulated (μΩ/Ω)	0.003	0.006	0.051	0.073	-0.039	-0.810
		Unc. (μΩ/Ω)	0.001	0.002	0.020	0.039	0.098	0.210
		Measured (μΩ/Ω)	-1.4	-0.8	-1.5	0.5	1.3	-0.3
		Unc. (μΩ/Ω)	9.2	9.2	9.2	9.3	9.8	10.4
10 A	0.06 Ω	Calulated (μΩ/Ω)	0.003	0.006	0.033	0.004	-0.460	-2.500
		Unc. (μΩ/Ω)	0.000	0.001	0.005	0.013	0.067	0.270
		Measured (μΩ/Ω)	-1.1	0.4	2.2	-2.4	-2.9	5.5
		Unc. (μΩ/Ω)	11.3	11.3	11.3	11.4	12.1	12.8

Table 4.Comparison of the measured ac-dc difference values (μΩ/Ω) of the original and new shunts generation.

Nominal current	Generation	Value	Frequency					
			500 Hz	1 kHz	10 kHz	20 kHz	50 kHz	100 kHz
30 mA	New	20 Ω	0	-1	2	3	5	7
	Original	50 Ω	-1	0	8	20	57	131
100 mA	New	6 Ω	-1	-2	1	3	4	6
	Original	10 Ω	1	-1	4	9	20	39
300 mA	New	2 Ω	1	1	1	2	4	6
	Old	3.3 Ω	0	0	4	7	13	22
1 A	New	0.6 Ω	-1	-1	-1	1	1	0
	Original	1 Ω	1	-3	-2	2	6	12
10 A	New	0.06 Ω	-1	0	-2	-2	-3	6
	Original	0.1 Ω	1	-1	-2	-3	-4	-23

Comparison of the calculated and measured values showed agreement better than 6 μΩ/Ω in the ac-dc difference at frequencies up to 100 kHz.

Future work will address the comparison of calculated and measured phase angle errors of the new shunts and the developing of high current shunts up to 100 A.

REFERENCES

[1] Garcocz, M.; Scheibenreiter, P.; Waldmann, W.; Heine, G., "Expanding the Measurement Capability for AC-DC Current Transfer at BEV," 2004 Digest of CPEM Conf, June 2004, pp.461,462.

[2] Pogliano, U., Bosco, G. C., Serazio, D., "Coaxial Shunts as AC–DC Transfer Standards of Current," IEEE Trans. on Instrum. and Meas., vol. 58, No.4, 2009, p. 872-877.

[3] Filipski, P.S.; Boecker, M., "AC-DC current shunts and system for extended current and frequency ranges," IEEE Trans. on Instrum. and Meas., vol.55, No.4, Aug. 2006, pp.1222-1227.

[4] Voljc, B.; Lindic, M.; Lapuh, R., "Direct Measurement of AC Current by Measuring the Voltage Drop on the Coaxial Current Shunt, " IEEE Trans. on Instrum. and Meas., vol.58, No.4, April 2009, pp.863-867.

[5] Voljc, B.; Lindic, M.; Pinter, B.; Kokalj, M.; Svetik, Z.; Lapuh, R., "Evaluation of a 100 A Current Shunt for the Direct Measurement of AC Current," IEEE Trans. on Instrum. and Meas., vol.62, No.6, June 2013, pp.1675-1680.

[6] K. Lind, T. Sorsdal, H. Slinde, "Design, Modeling, and Verification of High-performance ac-dc Current Shunts from Inexpensive Components," IEEE Trans. on Instrum. and Meas., vol. 57, No. 1, Jan. 2008, pp. 176-181.

[7] V. Nováková Zachovalová, "AC-DC current transfer difference in CMI," 2008 Digest of CPEM Conf., 2008, pp. 362-363.

[8] Zachovalová, V.N.; Šira, M.; Streit, J., "Current and frequency range extension of AC-DC current tranfer difference measurement system at CMI," 2010 Digest of CPEM Conf., 2010, pp.605,606.

[9] Zachovalova, V.N., "On the Current Shunts Modeling," IEEE Trans. on Instrum. and Meas., vol.63, No.6, June 2014, pp.1620-1627.